



## Robust Shape-based Matching Control of Robotic Conductive Charging Systems for Electric Vehicles

Bernhard Walzel<sup>1</sup> , Mario Hirz<sup>2</sup>  and Helmut Brunner<sup>3</sup> 

<sup>1</sup>Graz University of Technology, [bernhard.walzel@tugraz.at](mailto:bernhard.walzel@tugraz.at)

<sup>2</sup>Graz University of Technology, [mario.hirz@tugraz.at](mailto:mario.hirz@tugraz.at)

<sup>3</sup>Graz University of Technology, [helmut.brunner@tugraz.at](mailto:helmut.brunner@tugraz.at)

Corresponding author: Bernhard Walzel, [bernhard.walzel@tugraz.at](mailto:bernhard.walzel@tugraz.at)

### Abstract.

The increasing popularity of electric vehicles (EVs) and autonomous driving is calling for innovative user-centric and comfortable solutions for battery charging. Automated charging with standard connector technologies has the potential for offering high charging power by minimal EV- and infrastructure attachments as well as comfortable and safe charging processes. For realizing automated conductive (cable-based) charging via standard charging connectors and inlets, one challenge lies in the accurate position determination of the EV charging inlet, while interoperability and cost targets require to refrain from any vehicle adaptations or modifications to support the detection process. The present work introduces an accurate, robust and cost-efficient sensor system approach enabling both EV type detection and classification as well as the subsequent charging inlet position determination, based on 2D-cameras in combination with shape-based 3D-matching procedures. The system enables a robust inlet position determination of different vehicle types in various parking positions, while no adaptations on the vehicles are necessary. In this context, the paper provides insights into the sensor system development and highlights requirements on charging inlet detection, the recognition process of an Automated Conductive Charging System (ACCS) prototype as well as the evaluation of the introduced sensor system by experimental studies. The results of the presented work demonstrate the possibilities of charging electric vehicles autonomously by conductive charging standards.

**Keywords:** electric vehicle charging, robotics, shape-based 3D-matching, CAD shape models

**DOI:** <https://doi.org/10.14733/cadaps.2022.612-623>

## 1 INTRODUCTION

Automated Conductive Charging, either underbody (ACD-U-systems) or at the vehicle's side (ACD-S-systems) has the potential for offering high charging power as well as comfortable and safe charging processes. Designing ACD-S-systems with respect to interoperability with standardized charging inlets paves the way for further cost reduction and higher market potential, since existing charging standards, vehicles and infrastructure are compatible without any adaption. However, requirements on charging inlet position detection and robot control increase in their complexity. In this context, a new definition of ACD-S-systems is introduced: Automated Charging with Conductive Standards (ACCS) describes a side-coupling system, especially designed for fulfilling requirements on interoperability with standardized charging inlets, such as the Combined Charging System (CCS) [3] or Charge de Move (ChaDeMo) [4], can provide both, high customer comfort and safe operation. Standardized coupling systems are widely used and are able to transfer very high charging power. However, standardized charging cables and couplings are not designed for an automated connection. One of the difficulties lies in the accurate and robust charging inlet position detection and the provision of data for an exact control of the connector coupling process under consideration of robustness and cost demands, [20]. Previous works presented automated conductive charging concepts [16], [12] and [15]. However, no feasible solution for series application has been applied yet. Furthermore, the state-of-the-art analyses by market- and development-focused benchmarks as well as literature and patent research activities gave less information about a robust sensor system solution and functionality for charging inlet position identification [20].

One key role in the entire automated coupling and decoupling process can be seen in an adequate vehicle's charging inlet position detection, based on image recognition and CAD-data comparison. Actual developments in car-to-infrastructure communication (ISO 15118) [8] pave the way to wireless communication between vehicle and charging infrastructure. However, information about an exact position of the charging inlet is not expected to be provided by the vehicle, since it would need to gather the correct position in relation to the charging station within a tolerance of  $\pm 0.5$  mm, according to the state-of-the-art [20]. Therefore, in the present work, wireless vehicle-to-infrastructure communication is seen to have a potential to support the automated charging process (e.g. to register at the charging station, initialize and end the charging process or to proceed billing), while the actual charging inlet position determination is done without information from the vehicle.

Figure 1 shows an ACCS prototype that was developed during the research works. The prototype enables cable connection and disconnection at various mass production EVs via standard charging connectors. Particularly important for the functionality are the newly developed sensor technology, including 2D-cameras and CAD-shape models for vehicle classification and inlet position detection.



**Figure 1:** ACCS charging station prototype during outdoor tests.

## 2 PROBLEM DEFINITION

Figure 2, right, represents a charging lot and exemplary position frames of vehicle  $\{V\}$ , charging inlet  $\{I\}$ , parking lot  $\{R\}$  and the ACCS base  $\{A\}$ . The variable EV parking position  $\{V\}$  is characterized by translational and rotational position displacements in relation to  $\{A\}$ . An automated charging device has to compensate displacements between car and charging station by accurately determining the inlet's 3D-position (Figure 2, right,  $\{I\}$ ) in its 6 degrees of freedoms. For an actual application of standardized charging plugs, the sensor tolerance requirements are in an area of less than 0.5 mm in translational and 1.4 degree in rotational directions, as experimental investigations showed. These high requirements on position detection and robotics system control represent a serious challenge for the development of an automated charging station under reasonable cost boundaries. Figure 2, left and middle, shows the side view of an exemplary EV with open charging cap as well as a detail view of the CCS-Type-2 charging inlet. A cost-efficient sensor system is required to detect the vehicle and inlet without any vehicle adaptations, like additional markers. Different light situations and reflections might limit optical sensor technologies in their functionalities. The target of an interoperable ACCS, applicable to handle different EV types with different inlet positions and integration geometries, further increases the automation complexity [18].

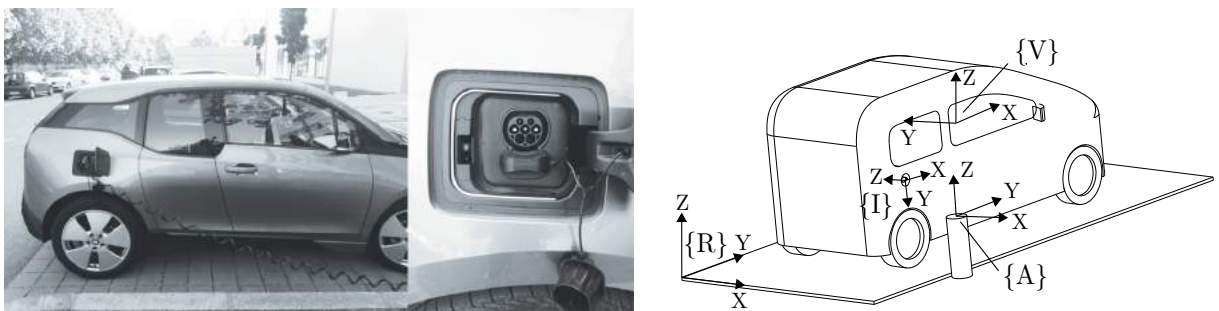


**Figure 2:** Left: Exemplary EV side view and detail view of an CCS-Type 2 charging inlet. Right: Exemplary representation of vehicle- and inlet positions at a charging lot, [18].

## 3 POSITION DETECTION PROCESS

In the present approach, 2D-cameras are used to maintain the required ACCS inlet- and vehicle detection accuracy, range and cost requirements and thus provide the basis for sensors selection [6]. The basic object recognition process is separated into three tasks, mainly responsible for vehicle classification, rough inlet position detection and a subsequent accurate inlet position detection. Figure 3 illustrates the entire vehicle- and inlet position recognition process. The process steps *Recognition I* and *Recognition II* are carried out by the same 2D-camera system and include *Vehicle recognition* as well as *Basic inlet position detection* and the *Charging start trigger*. An additional 2D-camera is responsible for the *Advanced inlet position detection* in the process step *Recognition III*. Both, vehicle classification and inlet 3D-position detection, are conducted by 2D-camera images and shape-based 3D-matching, [18].

Accurate and robust matching results require a suitable 3D-CAD model for the shape-based 3D-matching model generation. Therefore, shape-based 3D-matching uses contours, provided by a CAD-model of known objects, to estimate their position and orientation (pose) in a camera image [9]. Range and field of view depend on the application and can be specified. In course of the specific development, virtual cameras are placed around the 3D-object model, and the 3D-contour is projected into the lens plane of each camera position. In this way, the 3D-shape model stores 2D-representations for each view. In the matching process, the 2D-shape representations are used to find the best matching view. During the process, the object pose result is improved

step-by-step [10]. Matching is based on contour detection (edges) in an image. The stronger contours appear and are pronounced in an image, the better they can be captured.

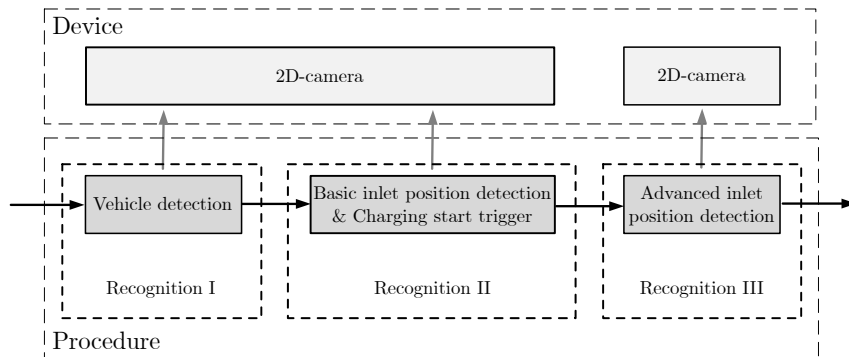


**Figure 3:** ACCS object recognition process including procedures for vehicle and inlet 3D-position detection [18].

*Recognition I* is responsible to gather information about the actual vehicle type to be charged. Figure 4, left, shows the charging socket and inlet sensor working range  $S_{CS}$ . In addition to the charging socket, the 2D-camera Field of View (FoV) covers the wheel fender. Fender- and charging cover area (Figure 4, right, F and CS) indicate striking geometric shapes and visible edges in a camera image. Two 2D-cameras observe the vehicle fender with its shapes and classify the vehicle by shape-based 3D-matching processes. If and after the vehicle is recognized and identified over its fender geometry, process steps for determination of  $\{I\}$  are initialized. The determination of  $\{I\}$  is done by the two subsequent process steps *Recognition II* and *Recognition III*. Field of view (Figure 5, FoV1, FoV2 and FoV3), position and orientation of each camera are positioned with respect to the ACCS component requirements and 2D-camera specifications.

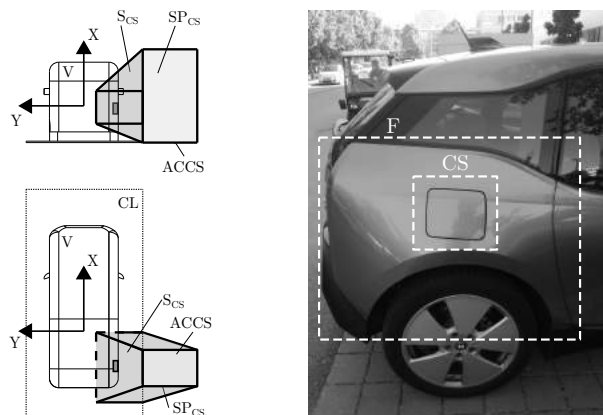


**Figure 4:** Left: Charging socket sensor working range concept. Right: 2D-image of a rear, right vehicle wheel fender and charging cover.

Camera 1 and Camera 2 (Figure 5, frame  $\{C1\}$  and  $\{C2\}$ ) are mounted on the ACCS and deliver necessary data for the process steps *Recognition I* and *Recognition II*. The position of Camera 2 is at the height of Camera 1 and extends the field of view in ACCS  $Y$ -axis (Figure 5, D1 and D2) to identify the vehicle fender. According to the ISO 15118 communication standard proposal, the charging start signal is initiated by the

vehicle by a communication channel to the charging station. This means that the vehicle, respectively the driver, has to initiate the charging process [8]. In case of the present prototype, the trigger to start charging is defined as the charging lid to be opened. In this way, the charging inlet is completely visible for Camera 1 and 2 and the charging process is started after recognition of an inlet shape. In case of "bad" lighting conditions, the frame Light Emitting Diodes (LED) (Figure 5, L) support the matching process by providing adequate light ratios. In the case of an unsuccessful detection, these are activated after a pre-defined time. For robot control in process step *Recognition III*, only the translational components  $X$ ,  $Y$  and  $Z$  of the frame  $\{I\}$  are of interest - the rotation components  $R_x$ ,  $R_y$  and  $R_z$  are not relevant. According to the camera specifications, the basic inlet position accuracy is given with 2.37 mm in horizontal (camera  $X$ -direction), 2.17 mm vertical (camera  $Y$ -direction) and 2.51 mm camera  $Z$ -direction. With the gathered charging inlet basic position information, the robot positions itself in front of the inlet within a short distance. During the process *Recognition III* Camera 3 (Figure 5, frame  $\{C3\}$ ) is responsible for the exact detection of  $\{I\}$ . In contrast to the previous process *Recognition II*, now the exact values of the  $X$ -,  $Y$ - and  $Z$ -coordinates and the  $R_x$ -,  $R_y$ - and  $R_z$ -rotations are from interest, for robot control [19].

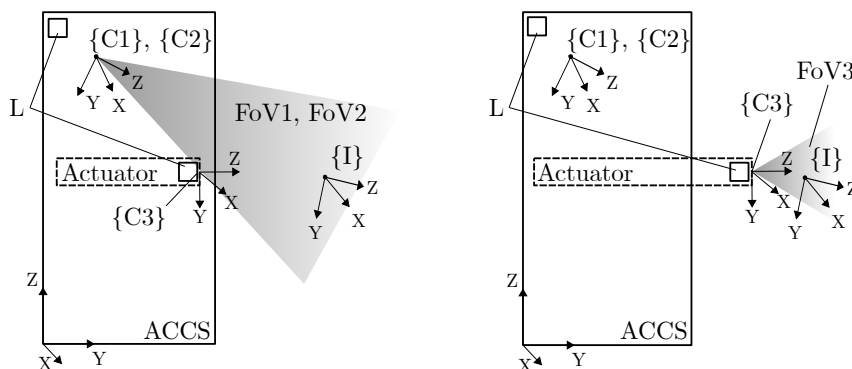


**Figure 5:** ACCS concept side view with an exemplary representation of an inlet frame and the field of view of the 2D-vision sensors. Left: Field of view of Camera 1 and Camera 2 at process step *Recognition II*. Right: Field of view of Camera 3 at process step *Recognition III*. [19]

### 3.1 Vehicle Detection

The charging process starts by checking the charging lot occupancy with Camera 1 and 2. In the present approach, the vehicle type classification is done by vehicle-specific distinctive contours and structures [6], [5] and shape-based 3D-matching. Figure 6 shows the rear right fender of the test vehicle BMW i3 as well as different views of the 3D-CAD model. This model serves as a template for the shape-based 3D-matching process, which is based on a database of rear wheel fenders of typical EVs. In this way, a match provides information about vehicle type and vehicle position on the charging lot. In this way, identification and classification are enabled without vehicle adaptations and additional communication, e.g. transmitter, RFID or sensor systems [18]. Optionally, registration and authentication of the vehicle type can be managed by wireless communication technologies [8].

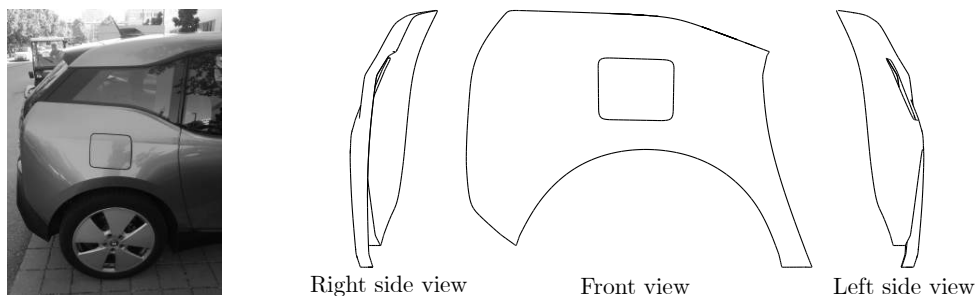


**Figure 6:** Left: Rear, right wheel fender of a BMW i3. Right: Different views of the BMW i3 fender 3D-CAD model for shape-based 3D-matching.

### 3.2 Inlet Detection

Successful and good matching results require a suitable 3D-CAD model for the shape-based 3D-matching model generation. For matching of the charging socket, one challenge includes the development of a universal interoperable 3D-shape-model for standardized charging inlets. In case of the CCS Type-2 inlet, the standard, [4] defines the geometrical shape of all parts (Figure 7, left, position 1), including DC connector (Figure 7, left, position 2) and socket frame (Figure 7, left, position 3) within the marked border (Figure 7, left, position 4), which is considered in the matching CAD-model. With this approach, the inlet position detection works without additional supporting attachments, e.g. markers, and does not require a change of the standardized geometry.

Enabling accurate matching results, the design of a sophisticated 3D-CAD matching model requires a detailed investigation of relevant and striking inlet edges and contours. Figure 7, right, shows detected edges along a diagonal line through the standard inlet by using the pixels of a greyscale camera image. The greyscale image with a colour depth  $T$  of 8 Bit/pixel possesses 256 values from 0 to 255. 0 defines the lowest grey value (minimum brightness, black), 255 the highest grey value (maximum brightness, white) [2].

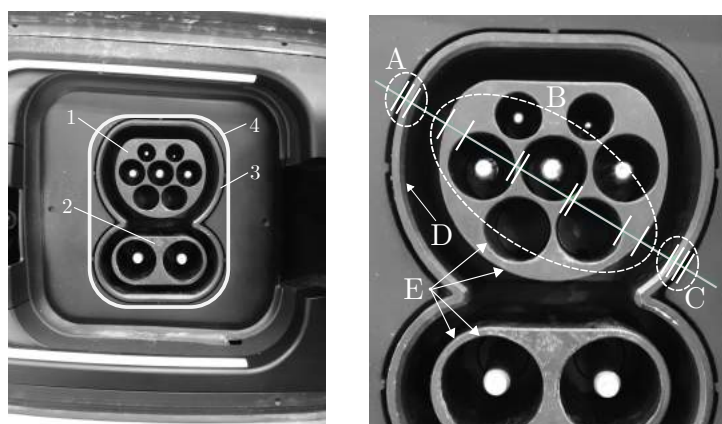


**Figure 7:** Left: Picture of a test vehicle's CCS Type 2 inlet. Right: Example of detected edges (orthogonal lines in relation to the examination line) by using grey value curve analyses.

The grey value function and its first derivation of the diagonal line (Figure 7, right) with a length of 875 pixels and a width of 2 pixels is shown in Figure 8. Both functions exemplary indicate the quality of the

inlet edge detection, and it is possible to develop a suitable matching model proposal on the basis of the edge detection results. However, different light and shadow conditions cannot be estimated completely. By a defined grey value derivation amplitude of  $\pm 20$  along the line, 15 edges (Figure 7, right) were found in the example. At region B and C (Figure 7, right), all edges along the defined line of the CCS Type-2 connector and the outer socket frame were successfully detected. At region A (Figure 7, right), the defined greyscale gradient was not reached, and the fourth edge was not detected (Figure 8, right). Reducing the gradient amplitude by  $\pm 5$  would detect the missing edge, but with the disadvantage that other unwanted edges or fragments would also be recognized. Only striking differences of grey values lead to good results. Light and shadow can have a significant influence on the image. Disturbing effects, e.g. edges disappearing by shadows, sloped or rounded geometric inlet surfaces due to different camera angles, distorted or blur edges, complicate a sophisticated edge detection.

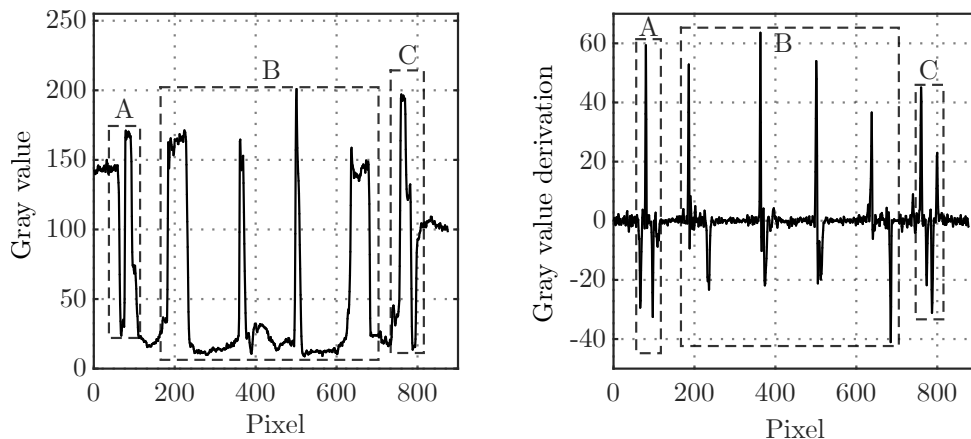


**Figure 8:** Left: Gray value function applied on a pixel examination line. Right: First derivation of the gray value function.

Furthermore, sloped surfaces or inlet shape deviations from the standard complicate the detection process and degrade matching results. As defined in the CCS-standard, shape tolerances for the socket frame are  $\pm 0.1$  mm at the  $1.1 \text{ mm} \times 45^\circ$  bevel (Figure 7, right, D) and  $\pm 0.1$  mm for the  $0.6 \text{ mm}$  radius at the CCS Type 2- and CCS DC-parts (Figure 7, right, E) [3]. Shapes with minimum contour deviations are represented at the 3D-CAD-model to reduce edge detection and light problems. The model was created by using the CCS Type 2 and CCS DC part (Figure 7 1, 2 and 3). The standard CAD drawings determine the inlet shape geometry dimensions [3]. The inlet front surface CAD-model has been converted to a 3D STL file-format for further processing by use of the vision software HALCON [10].

Figure 9, left, shows an inlet image during the process *Recognition III* in case of dark environmental light conditions. The image does not fulfil the defined matching process parameter limits, necessary for a functional and robust inlet position detection. For better results, light support is served by LEDs. Figure 9, right, shows the scene by light support of the robot head LED. The visibility of the inlets is improved significantly. However, light reflections on surfaces and edges (position 1 and 2) can occur and worsen the matching outcomes, as already mentioned, creating a field of tension in terms of visibility. Figures 9 show examples of inlet edge detection conditions due to shadows, dark light or reflections at two different vehicles types. In comparison to the clearly visible contours in Figure 9, left, the inlet of the other vehicle (Figure 9, left) is mounted deeper in the car body, which results in shadows. Due to the low contrast difference, it is challenging to detect edges, which makes additional spotlight necessary (Figure 9, right).



**Figure 9:** Examples of inlet camera images without and with LED light support.

#### 4 APPLICATION AND TESTING

The vision system was tested and evaluated under different test scenarios, including robustness and accuracy tests as well as different vehicles under indoor and outdoor conditions. Figure 10, left, shows the 3D-CAD surface-model including pre-defined reference coordinate system  $R_C$ . Position and orientation of the inlet in the captured camera image are related to  $R_C$ . An exemplary positive matching result and the corresponding inlet pose detection during tests are displayed in Figure 10, middle,  $M$  and  $\{I_M\}$ . The points lie on the height of the inlet pin-wholes and -edges in inlet's  $Y$ -direction. Selection of the correct CAD-model from the database relies on the preceded correct vehicle classification at the beginning of the matching process (Figure 10, right).

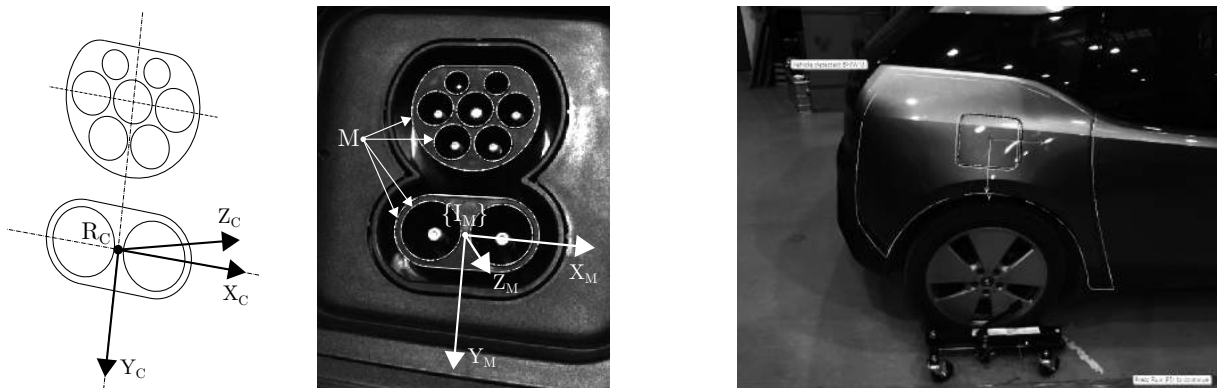


**Figure 10:** Left: CAD-model as template for shape-based 3D-matching and matching result of an image from the robot-head mono camera. Right: Exemplary positive matching result of model an vehicle type.

##### 4.1 Robustness Tests

The test series aim was to determine the inlet position detection and charging cable control robustness at different vehicle positions. The test examined the robot behaviour at the maximum working range and with large vehicle positioning angle offsets of up to  $\pm 15^\circ$ . Additionally, the height of the vehicle varied during the charging tests by different loading situations (position of the inlet regarding the robot  $Z$ -axis). The high variation of the inlet position by varying the number of vehicle occupants contributed to the evaluation of the



robustness of the recognition and control approach. Figure 11, left, exemplarily depicts the relative position of vehicle  $\{V\}$  and inlet  $\{I\}$  in relation to the robot base  $\{B\}$  with an angular offset of  $15^\circ$ . In the course of this test series, a total of 42 experiments with 6 basic positions with 7 angular offsets, each from  $-15^\circ$  to  $+15^\circ$  with  $5^\circ$  interval were carried out in the robot working area (Figure 11, right). For the evaluation of the prototype function, the charging process was divided into 5 steps [19]:

1. Docking (connector positioning in front of the charging inlet)
2. Plug-in until the end position of the charging inlet
3. Plug-out
4. Closing of the charging lid
5. Robot moving to the waiting position

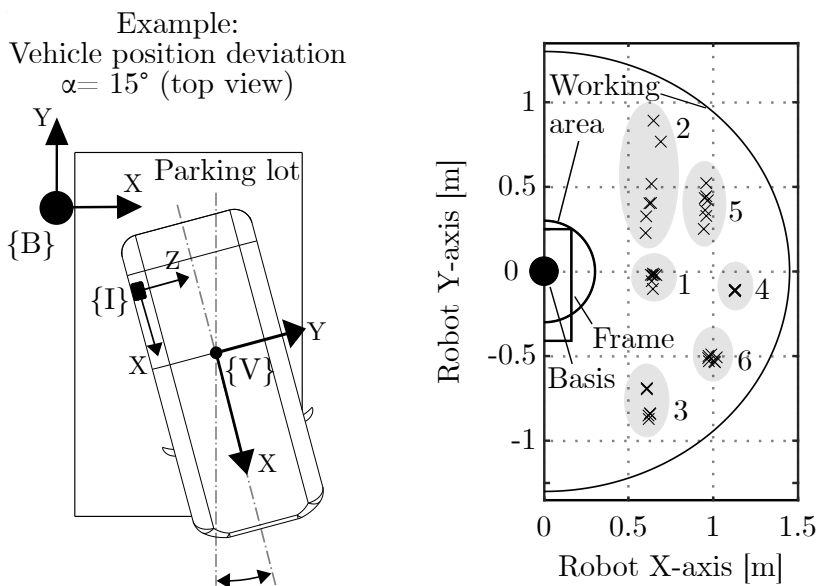


**Figure 11:** Left: Exemplary presentation of the vehicle position with  $15^\circ$  angular deviation. Right: Representation of the inlet test positions to evaluate the robustness of the charging station vision system [19].

The test results are shown in Table 1. Docking, plug-in, plug-out as well as moving to the waiting position were carried out successfully in all 42 tests. Just two times, on test position 3, at  $10^\circ$  and  $15^\circ$  vehicle rotation angle in relation to the robot  $Z$ -axis, the charging lid was not sufficiently closed until its end position. The charging station linear actuator, that is responsible for the charging lid closing, could not completely close the lid due to its high relative position deviation. The inlet position regarding the robot  $X$ - and  $Y$ -axis were specified by the robot range limits and the angle deviation of the vehicle. That is why the inlet position varies along with the robot  $Y$ -axis, that is particularly visible at test basic position 2 (Figure 11, right). In robot  $Z$ -axis the inlet mean position regarding the robot base was recorded with 52.64 cm with a standard deviation of 4.6 mm. This result shows the essential change in the height of the vehicle, which must not be neglected in the design of an automated charging system. The test shows, that even if the accuracy of the position sensor system decreases with increasing vehicle parking angles relatively to the robot system, the tests were carried out successfully with a high level of robustness [19].

**Table 1:** Summary of the robustness experiment results [19].

Step number	Step	Result	Annotation
1	Docking	42 times successful	-
2	Plug-in	42 times successful	-
3	Plug-out	42 times successful	-
4	Charging lid closing	40 times successful	2 × incorrect positioning of the actuator
5	Robot moving to waiting position	42 times successful	-

## 4.2 Vehicle Classification and Inlet Position Detection Experiments with Different Vehicles Including Parking Procedure

Further test series comprised the entire automated charging process, including driving in and parking the vehicle, recognition of vehicle and inlet by the vision system, plug-in and plug-out of the charging cable and leaving the charging station.

Vehicle classification and inlet detection tests have been carried out with 5 different test vehicles [1], [7], [13], [17]. The test vehicle types, its charging inlet locations and protection as well as test results are shown in table 2. Test drivers parked the vehicles for- and backwards on the charging lot. The charging lot was marked with adhesive tapes to simulate a parking lot with typical dimensions [11]. Practised and unpractised drivers directed the test vehicles to the charging station and parked the car near the charging station, according to their judgment without vehicle parking positioning aids. During the test series, success rate of vehicle classification and inlet position determination was between 75% and 95%. Furthermore, test series included a mass production EV with an inlet, basically CCS Type-2 compatible but not standardized [14]. Here the main difference was a curved surface in contrast to the standardized flat one. To address this issue in the matching process, an additional CAD-model, bent by the defined curvature, has been implemented.

**Table 2:** ACCS prototype test EVs [19].

Test vehicle	Type	Year	Security cap	Plug position and -height [cm]	Vehicle classification and inlet position detection success rate
1	BMW i3 60 Ah	2016	Plastic flap	Rear, right, 95	95%
2	BMW i3 94 Ah	2017	Plastic flap	Rear, right, 95	95%
3	VOLKSWAGEN e-Golf	2019	No flap	Rear, right, 88	80%
4	HYUNDAI IONIQ Electro	2019	No flap	Rear, left, 97	90%
5	TESLA Model 3	2019	No flap	Rear, left, 95	75%

## 5 CONCLUSIONS

The presented work introduces a new approach for accurate and cost-efficient object detection for automated charging of electric vehicles with conductive standards by combination of CAD-based model provision and 2D-camera-based object recognition. The introduced sensor system does not require adaptation of the charging inlets to enable the inlet position detection. In this way, the vision system has been successfully tested with non-modified standardized CCS Type-2 vehicle inlets and different vehicle types. The charging inlet position detection approach can also be applied to different inlet designs, standardized (e.g. Type-2 or ChaDeMo) or even not standardized. The results support a further development of ACCS, opening advantageous possibilities to guide robot-controlled systems for automated charging of different electric vehicle types with a high robustness of operation.

## ACKNOWLEDGEMENTS

The authors want to express their acknowledgement to the project partners BMW AG, MAGNA Steyr Engineering, KEBA AG, Austrian Society of Automotive Engineers (OEVK) and the Department of Computer Science and Engineering at the University of South Florida (USF) for the excellent cooperation. In addition, thanks goes to the Austrian Research Promotion Agency (FFG) and the Austrian Federal Ministry of Transport, Innovation and Technology (bmvit) for funding.

*Bernhard Walzel*, <http://orcid.org/0000-0003-4818-3726>

*Mario Hirz*, <http://orcid.org/0000-0002-4502-4255>

*Helmut Brunner*, <http://orcid.org/0000-0003-1739-8214>

## REFERENCES

- [1] BMW: Technical data BMW i3 and BMW i3s, date of access: 03/12/2016. <https://www.bmw.de/de/neufahrzeuge/bmw-i/i3/2017/technische-daten.html#tab-0>.
- [2] Burger, W.; Burge, M.: Digitale Bildverarbeitung: Eine algorithmische Einführung mit Java. Springer Vieweg, Berlin and Heidelberg, 3. Edition, 2015. <http://doi.org/10.1007/978-3-642-04604-9>.
- [3] Comission, I.E.: IEC 61851-23:2014: Electric vehicle conductive charging system - Part 23: DC electric vehicle charging station. International Standard, 2014.
- [4] Comission, I.E.: IEC 62196-3:2014: Plugs, socket-outlets, vehicle connectors and vehicle inlets - Conductive charging of electric vehicles - Part 3: Dimensional compatibility and interchangeability requirements for d.c. and a.c./d.c. pin and contact-tube vehicle couplers. International Standard, 2014.
- [5] Gulanova, J.; Gulan, L.; Forrai, M.; Hirz, M.: Generative engineering design methodology used for the development of surface-based components. In Computer-Aided Design and Applications, Volume 14, 2017. <http://doi.org/10.1080/16864360.2016.1273581>.
- [6] Hirz, M.; Walzel, B.: Sensor and object recognition technologies for self-driving cars. In Computer-Aided Design and Applications, Volume 15, 2018. <http://doi.org/10.1080/16864360.2017.1419638>.
- [7] HYUNDAI: Technical data and specifications HYUNDAI IONIQ Electro. Available at <https://www.hyundai.at>, date of access: 05/06/2019. <https://www.hyundai.at>.
- [8] International Standard Organization: ISO 15118-1: Road vehicles - vehicles to grid communication interface, Part 1-8., 2018.
- [9] Jayawardena, S.; Hutter, M.; Brewer, N.: A novel illumination-invariant loss for monocular 3d pose estimation. In 2011 International Conference on Digital Image Computing: Techniques and Applications, 2011. <http://doi.org/10.1109/DICTA.2011.15>.
- [10] MVTec Software GmbH: HALCON Vision Software - Version 13.0.1. <https://www.mvtec.com>, 2017.
- [11] Pech, A.; Jens, K.; Warmuth, G.; Zeininger, J.: Parkhäuser - Garagen: Grundlagen, Planung, Betrieb, 2. Edition, Volume 18. Springer, Vienna, 2009. <http://doi.org/10.1515/9783990432815>.
- [12] Tesla: Charger prototype finding its way to model s, date of access: 03/10/2015. <https://www.youtube.com/watch?v=uMM01RfX6YI>.
- [13] TESLA: TESLA homepage, date of access: 05/05/2020. [https://www.teslamotors.com/de\\_AT/models](https://www.teslamotors.com/de_AT/models).
- [14] TESLA: TESLA Model 3, date of access: 05/05/2020. [https://www.teslamotors.com/de\\_AT/models](https://www.teslamotors.com/de_AT/models).
- [15] University of Technology Dortmund: University of Technology Dortmund: Ladesystem der TU-Dortmund betankt Elektroautos automatisch. <http://www.e-technik.tu-dortmund.de>, date of access: 03/10/2015.

- [16] VOLKSWAGEN: E-smartconnect: Volkswagen is conducting research on an automated quick-charging system for the next generation of electric vehicles, date of access: 03/10/2015. <https://www.volkswagen-newsroom.com/>.
- [17] VOLKSWAGEN: Technical data and specifications VOLKSWAGEN e-Golf., date of access: 03/10/2019. <https://www.volkswagen.at/e-golf/infomaterial>.
- [18] Walzel, B.: Automated Charging of Electric Vehicles with Conductive Standards. Ph.D. thesis, Institute of Automotive Engineering, Graz University of Technology, 2020.
- [19] Walzel, B.; Hirz, M.; Brunner, H.: Robot-based fast charging of electric vehicles. In In WCX SAE World Congress Experience. American Society of Mechanical Engineers, 02/04/2019, Michigan. <http://doi.org/https://doi.org/10.4271/2019-01-0869>.
- [20] Walzel, B.; Sturm, C.; Fabian, J.; Hirz, M.: Automated robot-based charging system for electric vehicles. In 16th International Stuttgart Symposium. Springer, 2016. [http://doi.org/DOI:10.1007/978-3-658-13255-2\\_70](http://doi.org/DOI:10.1007/978-3-658-13255-2_70).